JOURNAL OF Applied Polymer SCIENCE

# Studies on the Surface Properties of Mixed-Matrix Membrane and Its Antifouling Properties for Humic Acid Removal

**Y. H. Teow, A. L. Ahmad, J. K. Lim, B.S. Ooi**
School of Chemical Engineering, Engineering Campus, Universiti Sains Malaysia, Seri Ampangan, 14300 Nibong Tebal, Penang, Malaysia
Correspondence to: B.S. Ooi (E-mail: chobs@eng.usm.my)

**ABSTRACT:** A major factor limiting the use of ultrafiltration (UF) membrane in water treatment process is the membrane fouling by natural organic matter such as humic acid (HA). In this work, neat PVDF and PVDF/$TiO_2$ mixed-matrix membranes were prepared and compared in terms of their antifouling properties. Two commercial types of $TiO_2$ namely PC-20 and P25 were embedded to prepare the mixed matrix membranes via *in situ* colloidal precipitation method. The contact angles for the mixed-matrix membranes were slightly reduced while the zeta potential was increased (more negatively charged) compared with the neat membrane. Filtration of HA with the presence of $Ca^{2+}$ demonstrated that mixed-matrix membrane could significantly mitigate the fouling tendency compared with the neat membrane with flux ratio ($J/J_0$) of 0.65, 0.70, and 0.82 for neat PVDF membrane, PVDF/$TiO_2$ mixed-matrix membrane embedded with P25 and PC-20, respectively. PC-20 with higher anatase polymorphs exhibited better antifouling properties due to its hydrophilicity nature. © 2012 Wiley Periodicals, Inc. J. Appl. Polym. Sci. 000: 000–000, 2012

**KEYWORDS:** membranes; nanoparticles; nanowires and nanocrystals; particle size distribution; phase separation

Received 4 January 2012; accepted 18 August 2012; published online
**DOI: 10.1002/app.38494**

## INTRODUCTION

Polyvinylidene fluoride (PVDF) is one of the most extensively applied membrane materials in the industry. However, PVDF UF membrane with its relatively hydrophobic nature limits its application in water separation process as they exhibit lower permeation flux due to the high surface tension between water and the membrane surface and more susceptible to fouling. Fouling caused by natural organic matter (NOM) is a major obstacle for efficient use of ultrafiltration (UF) membranes in the water purification process. Fouling could greatly reduces the permeate flux and increasing the operational pressure, which leads to a higher operational cost, and a short membrane lifespan. Several studies had demonstrated that humic acid (HA), which is an important forebonding of trihalomethane and haloacetic acids, has a major influence on membrane fouling in the application for water treatment.[1,2] HA exists ubiquitously in the aquatic environment which primarily results from the microbiological degradation of surrounding vegetation and animal decay that enter surface water through rain water run-off from the surrounding land.[3] Humic acid are thought to be the complex aromatic macromolecules owing to the presence of both aromatic and aliphatic substances with three main functional groups: carboxylic acids (COOH), phenolic alcohols (OH), and methoxy carbonyls (C=O).[4]

The effects of solution chemistry that plays an important role on HA fouling were broadly investigated in several membrane processes.[5–7] The charge and configurations of HA macromolecules is extensively affected by its solution chemistry, which could alter the structure and hydraulic resistance of the foulant deposit layer. Wang et al., Hong et al. studied the effect of solution chemistry on membrane fouling in the treatment of water solutions containing HA. The results showed that the $CaCl_2$ or $MgCl_2$ salts could readily form complexes with the functional groups of humic macromolecules, increase the electrostatic shielding among the charged HA molecules and change the charge of both humic substances and membrane surface thus caused more severe fouling.[3,5,8]

A variation in membrane properties such as pore size, surface charge and hydrophilicity might affect the physic-chemical interactions of membrane and its solution.[9] In the previous study, Kabsch-Korbutowicz et al. investigated the deterioration of permeate flux during the UF of HA and found that hydrophobic UF membranes were more susceptible to HA fouling than hydrophilic UF membranes.[7] This finding was in line with the work of Lee et al.[10] who found that the hydrophilic regenerated cellulose membranes has superior antifouling property compared to the hydrophobic polyethersulfone membranes.

Recently, the combination of $TiO_2$ nanoparticles (NPs) with membrane filtration has been widely reported for its antifouling properties.[11,12] In addition to hydrophilic characters, membranes which possessed a negative charge on the top selective layer were also found extra useful in lowering fouling propensity.[13] Kwak et al. reported that the deposition of $TiO_2$ NPs into hand-cast polyamide composite membrane had made an obvious difference in both hydrophilicity and flux.[14] Among the technical innovations used to incorporate $TiO_2$ NPs into the membrane polymeric matrix, addition of $TiO_2$ NPs during coagulation precipitation is considered as one of the most convenient methods to create the impact on membrane hydrophilicity.

Because of the complex chemical and physical interactions (fouling) in the UF process for water solutions containing HA, a more systematic investigation of these interacting aspects is needed. The main objective of this article is to evaluate the effects of membrane surface chemistry on membrane fouling via NPs modification.

## EXPERIMENT

### Materials

PVDF (Solvay Pharmaceuticals) ultrafiltration membranes were prepared by casting the PVDF in *N*-*N*-dimethylacetamide, DMAc (Merck, Germany) (Assay (GC, area %) $\geq$ 99%) solution at 200 $\mu$m thickness. Two different types of commercial titanium dioxide, $TiO_2$ nanopowder were purchased from TitanPE Technologies, China (trade name: PC-20; particle size of 20 nm) and Sigma-Aldrich, St. Louis, MO (trade name: P25; particle size $\sim$ 21 nm). As reported by the manufacturer, PC-20 contains about 85% anatase and 15% rutile, while P25 contains about 75% anatase and 25% rutile. They were used as received.

Synthetic HA obtained from Sigma-Aldrich was used as the organic foulant during the experiment without further purification. Sodium hydroxide, NaOH solution was used to improve the dissolution of HA in water. Feed solutions were prepared by dissolving a preweighed 10 mg of HA powder in 5 L of distilled water. The solution pH was adjusted to pH 7 by addition of small quantities of 0.1*M* NaOH. To study the effect of HA fouling, the analytical grade inorganic salt ($CaCl_2$) was used to adjust the total ionic strength of the HA feed solution.

### Preparation of Stable $TiO_2$ Suspension

Chemical and mechanical treatments were carried out to enhance the $TiO_2$ colloidal stability in the coagulation bath as described below.

**Chemical Method.** First, in order to increase the stability of the $TiO_2$ particles in distilled water, the chemical modification of the original $TiO_2$ nanopowder was carried by adjusting the pH value of the $TiO_2$ suspension. Hydrochloride acid solution (HCl) was added drop-wise and mechanically stirred until it reaches equilibrium of pH 4.0 to achieve electrostatic stability (zeta potential $> +30$ mV). The pH value of the $TiO_2$ suspensions was measured using a pH meter (Eutech Instruments).

**Mechanical Method.** The $TiO_2$ cluster was further broken down by subjecting the $TiO_2$ solution to 15 min ultrasonic irradiation using Telsonic ultrasonic horn (SG-24-500P, Telsonic Ultrasonics). The frequency of the ultrasound was kept constant at 18.4 kHz.

### Membrane Formation and *In Situ* Particle Embedment

The membrane casting solutions were prepared by dissolving predried PVDF (24 h oven dried at 70°C) using DMAc in a 200-mL beaker. Composition of the PVDF/solvent solutions was kept constant at 18:82 in weight percentage.

To obtain complete dissolution and optimal dispersion of the polymer solution, the mixture was subjected to an initial constant stirring of 250 rpm at 65°C for 4 h to form a homogenous solution. The homogenous membrane polymer solution was then left overnight under stirring at 40°C and then kept in a centrifuge tube. The trapped air bubbles were removed by standing the solution overnight. Solvent loss by evaporation was negligible due to the high boiling point of DMAc at 164–166°C.

The polymer solution was cast using a thin film applicator (Elcometer 4340, Elcometer (Asia) Pte) on a flat glass plate wrapped with nonwoven polyester fabric (Holleytex 3329, Ahlstrom) to form a film at nominal thickness of 200 $\mu$m. The polyester fabric acts as membrane support layer, providing mechanical strength to the membrane for pressure resistant. Thereafter, the nascent membrane on the glass plate was solidified by immersion into a precipitation water (distilled water) bath immediately to avoid excessive surface evaporation. The immersion was left for a day to ensure complete solidification and removal of residual solvent from the membranes. The resulting fabricated membrane was recovered from the coagulation bath after detaching from the glass plate and subsequently rinsed with and soaked in a bath of fresh distilled water. Drying was sequentially done after dipping the membrane in ethanol to avoid microbial growth.

To introduce $TiO_2$ particles on the membrane surface, the casted nascent PVDF membrane on the glass plate was immersed into 0.001 g/L $TiO_2$ colloidal suspension as prepared by using the method stated in Section 2.2. Since the membrane surface solidification and particle embedment occur simultaneously, this particle incorporation method is an *in situ* approach to embed particles onto the membrane surface.

### Membrane Characterization

**SEM Analysis.** Top surfaces morphology of the PVDF/$TiO_2$ mixed matrix membranes was observed using a Field Emission Scanning Electron Microscope (FESEM) (SUPRA 35 VP, Carl Zesis). For FESEM observation, the membrane samples were cut into appropriate size and mounted on the sample holders. K 550 sputter coater was used to coat the outer surface of the membrane sample with a thin layer of gold under vacuum to provide electrical conductivity. After gold/palladium sputtering, the samples were examined under the electron microscope at potentials of 10.0 kV. Using the same sample in SEM, the surface composition analysis including quality of dispersion and existence of $TiO_2$ particles on the membrane surface were carried out using energy dispersive X-ray (EDX) (EDAX).

**Pore Size Distribution.** Pore size of the membranes was determined using gas flow/liquid displacement method via Capillary

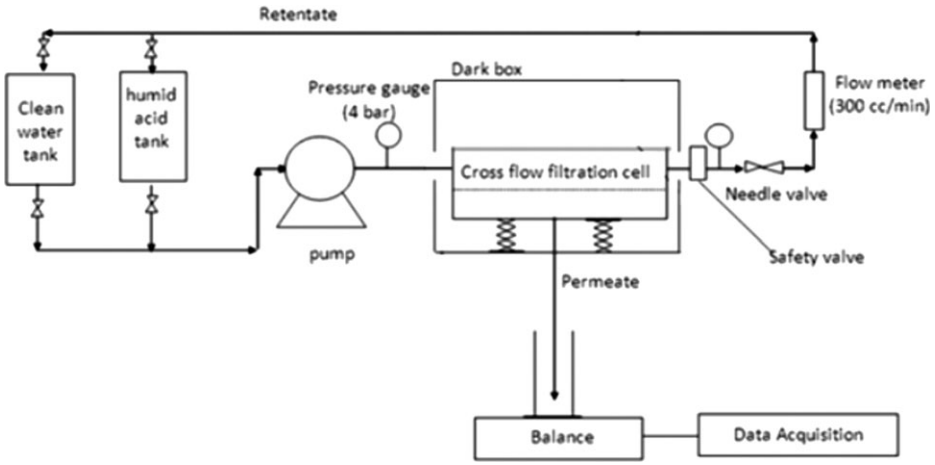


**Figure 1.** Schematic diagram of cross-flow recirculation membrane filtration rig.

Flow Porometer Porolux 1000 (Benelux Scientific, Germany). Membrane samples with diameter of 10 mm were characterized using the "dry up-wet up" method. In this method, gas flow was measured as a function of transmembrane pressure, initially through wetting of membrane with 1,1,2,3,3,3-haxafluoropropene followed by dry flow of gas through the membrane. The pore size distribution was estimated using PMI software.

**TgA.** The thermal stability and degradation of PVDF/$TiO_2$ mixed matrix membranes was examined by Thermal Gravitational Analysis (Perkin Elmer, USA) performed by a means of TGA 7 Thermogravimetric Analyzer. Aluminum open pans were used as sample holders. A membrane sample was placed on a pan by means of a plastic syringe in order to keep the sample mass and shape as uniform as possible. The sample mass weighing approximately 5–7 mg was used. Degradation temperatures were determined by heating the membrane sample using pure oxygen under ambient pressure at a heating rate of 20°C/min for the temperature range of 30–850°C and observing regions of significant weight loss. The $TiO_2$ concentration on membrane surface was estimated from the residual weight.

**Surface Tension (Wettability) Measurement.** The membrane wettability is characterized by static contact angle method based on sessile drop technique using a DropMeter A-100 contact angle system (Rame-Hart Instrument). The membrane sample was stuck onto a glass slide using double-sided tape to ensure its top surface was upward and flat. A droplet (~13 μL) of deionized water was dropped onto the dry membrane surface using a microsyringe at room temperature (21 ± 1°C). Immediately, a microscope with long working distance 6.5 × objectives was used to capture micrographs at high frequency (100 Pcs/s). The reported contact angles were average values from the measurements taken at 10 different locations on the membrane surface, as a measure to minimize random error.

**Streaming Potential.** The surface properties of the membranes were examined using streaming potential device. The streaming potential was evaluated using a devise constructed from two Plexiglas chambers with Ag/Ag/Cl electrodes inserted at each end. Data were obtained using 10 m*M* NaCl at pH 7.0, with the fluid flow across the membrane surface. The apparent zeta potential ($\xi$) was evaluated from the slope using the Helmholtz-Smoluchowski equation

$$\xi = \left(\frac{\eta \Lambda_o}{\varepsilon_o \varepsilon_r}\right) \frac{dE_z}{d\Delta P} \quad (1)$$

where $\Lambda_0$ is the solution conductivity, $\eta$ is the absolute viscosity of medium, $\varepsilon_0$ is the permittivity of vacuum, and $\varepsilon_r$ is the dielectric constant of the medium.

As streaming potential is linearly dependent on the applied pressure differential, it allows apparent zeta potential to be evaluated directly from eq. (1). Several studies have shown that eq. (1) provides useful information on the charge characteristics of membranes even though the Helmholtz-Smoluchowski equation neglects the effects of surface conductance and overlapping double layers. All results in this study were reported in terms of apparent zeta potential data as calculated from eq. (1).

### Crossflow Filtration

Figure 1 displays the schematic diagram of the experimental set up for crossflow filtration. The rig mainly consist of a membrane cross-flow filtration cell, feed reservoir (HA tank and clean water tank), peristaltic pump, flow meter for measuring flow rate, balance for measuring filtrate flow with data acquisition system, pressure gauge to show the equilibrium pressure and to evaluate the membrane performance under different pressure. All produced flat sheet membranes were cut into the disc shape and laid on top of the membrane holder in a designed stainless steel circular membrane test cell with a diameter of 5.1 cm (effective membrane filtration area of 20.43 $cm^2$ excluding the area cover by the O-ring) and tightened by a rubber O-ring.

Before the experiment was carried out, the membrane was compressed using distilled water at constant pressure of 1.0 bar for 1 h and left for a day. During the experiment, the synthetic HA solution was charged into a 3 L feed tank and recirculated at a

constant cross-flow rate per unit projection membrane area of 0.04 L/min using the peristaltic pump (Hydra-Cell, Wanner International). Filtration pressure was generated using a peristaltic pump and controlled by a needle valve at 0.5 bar while the permeate side was opened to the atmosphere. The retentate was returned to the feed tank (HA tank) to minimize the changes of feed concentration. Fresh feed solution was added every 2 h in order to maintain constant concentration. Permeate flux was measured every 1 min by weight differences obtained online from the analytical balance.

## RESULTS AND DISCUSSIONS

### Morphologies of PVDF/$TiO_2$ Mixed Matrix Membrane

Figure 2 shows the SEM top surface images of PVDF/$TiO_2$ mixed matrix membranes for membranes prepared using DMac as solvent immersed into different type of commercial $TiO_2$ colloidal suspension containing 0.001 g/L $TiO_2$ NPs. It can be seen from Figure 2 that connected pore structure appeared on the surface of PVDF membrane using DMAc as solvent and the type of commercial $TiO_2$ nanopowder used does not contribute to the structural change of membrane morphology due to its similar kinetic and thermodynamic environment during phase inversion.

In this colloidal precipitation method, $TiO_2$ nanoparticles were introduced into the whole membrane matrix during solvent exchange process as reported in our previous works.[15] This can be proven by the cross-sectional SEM images as well as the EDX line mapping in Figure 3. As apparent from the figure, the titanium line scanning of both mixed matrix membrane shows a uniform and similar distribution pattern which had proven the embedment of $TiO_2$ NPs in the membrane matrix, indicating that the polymer is homogeneously embedded with the $TiO_2$ NPs. However, the titanium signal recorded for membrane prepared by 0.001 g/L PC-20 was much more uniform compared to 0.001 g/L P25. Therefore, it can be ruled out that this was caused by higher degree of aggregation of PC-20 during the *in situ* precipitation process, produces membrane with poorer particle size distribution.

Sizes of NPs distributed on the PVDF/$TiO_2$ mixed matrix membrane surface were measured from the FESEM images using ImageJ 1.43 u software at 10.00 k× magnification, and the results are presented in Figure 4. Figure 4 shows that different type of commercial $TiO_2$ nanopowder did play an important role in changing the particle size distribution on the membrane surface. Membranes using P25 as colloidal suspension produced smaller surface particles compared with the systems using PC-20. This phenomenon is probably due to the higher agglomeration tendency of PC-20 compared to P25 which promote particle aggregation during the phase inversion. The increasing deposition of $TiO_2$ particles on membrane surface will likely provide additional hydrophilicity strength to the membrane, possibly increasing the permeate water flux and its antifouling properties.

### Pore Size Distribution

Pore size distributions of the neat and PVDF/$TiO_2$ mixed-matrix membrane were shown in Figure 5. As can be seen from Figure 5, all the membranes prepared had quite similar pore size distribution. The maximum number of pore, $r_{p,max}$ for the neat and mixed-matrix membrane is around 0.05 $\mu$m whereas the pore size distribution was slightly wider for mixed-matrix membrane prepared via *in situ* colloidal precipitation method. By adding $TiO_2$ NPs into the membrane polymeric matrix, it induced the bigger pores; this is probably due to the seeding

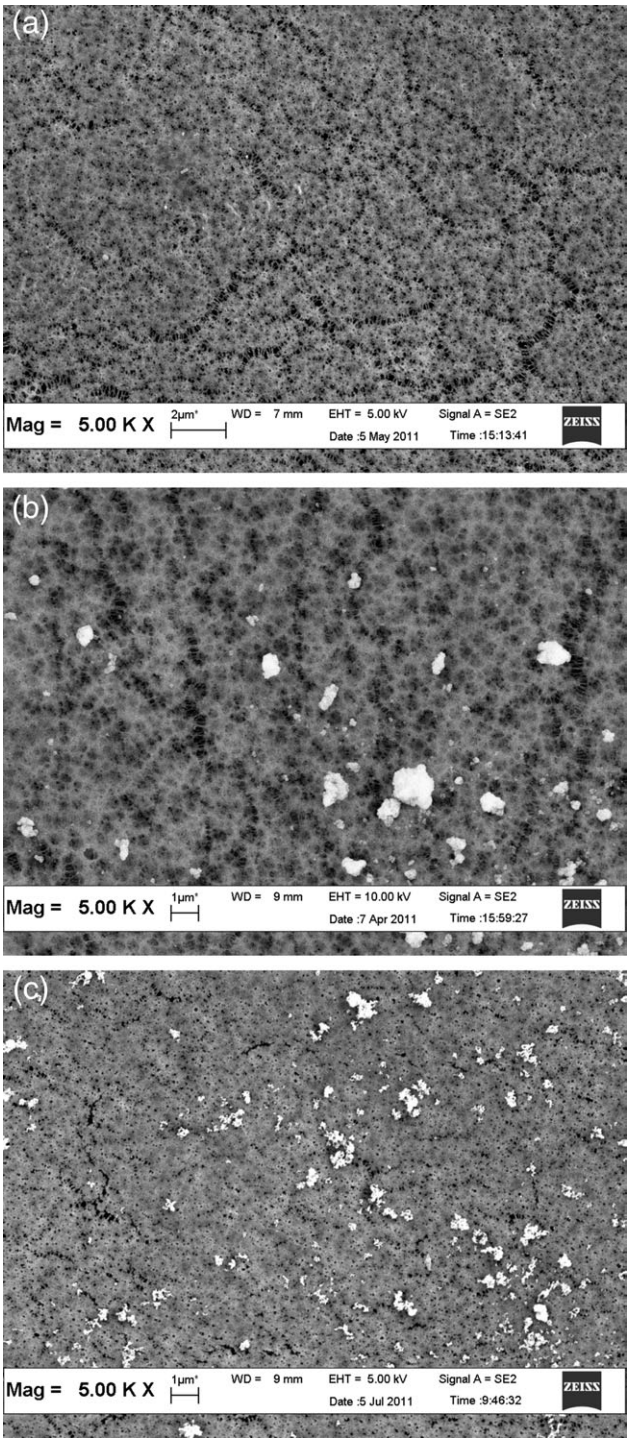


**Figure 2.** FESEM micrographs reveal detail of topography structure of PVDF/$TiO_2$ mixed matrix membrane (a) neat (b) 0.001 g/L PC-20 (c) 0.001 g/L P25.

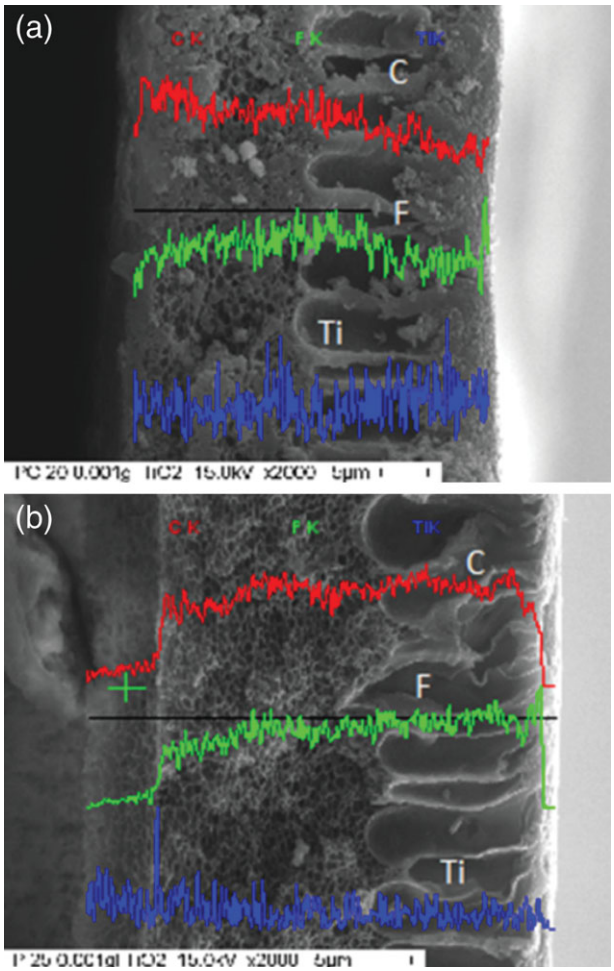


**Figure 3.** The $TiO_2$ distribution pattern on PVDF/$TiO_2$ mixed matrix membrane immersed in (a) 0.001 g/L PC-20 (b) 0.001 g/L P25. [Color figure can be viewed in the online issue, which is available at wileyonlinelibrary.com.]

effect of fine NPs which induced the early vitrification of the polymer. As a result bigger pores were produced. However, the increase of membrane pore size of was not significant indicating that colloidal precipitation method is an ideal method to prepare membrane with minimum changes to its physical properties.

### TgA

The TGA analysis of PVDF/$TiO_2$ mixed matrix membrane with $TiO_2$ concentration of 0.001 g/L before and after undergoes 6 h of pure water flux filtration process was reported in Figure 6. Neat PVDF membrane is almost fully decomposed when the samples heated up to 850°C in oxygen atmosphere. Thus, titanium was the main component of the residual of PVDF/$TiO_2$ mixed matrix membranes. According to the TGA results in Figure 6, after thermal decomposition at 850°C, the residual weight percent of titanium particles in membrane prepared before and after 6 h of membrane filtration process for both 0.001 g/L of P25 and PC 20 $TiO_2$ were almost the same ranging from 3 to 4 wt %. These results indicated that the high stability of $TiO_2$ NPs on PVDF matrix was obtained due to the hydrogen

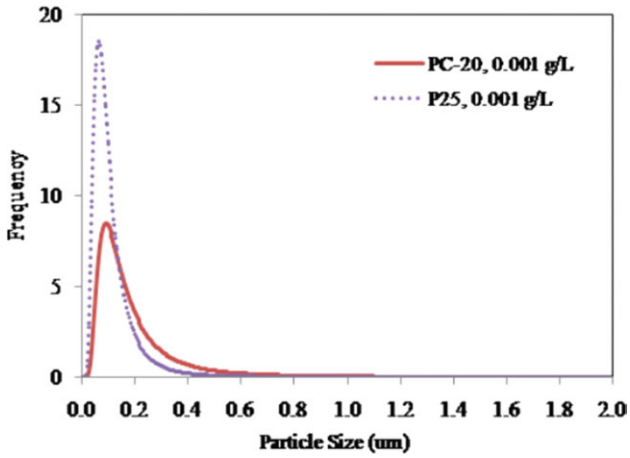


**Figure 4.** $TiO_2$ particle size distribution on the PVDF/$TiO_2$ mixed matrix membrane. [Color figure can be viewed in the online issue, which is available at wileyonlinelibrary.com.]

bonding between fluoride of PVDF and the partially hydroxylised $TiO_2$ surface.[15]

### Contact Angle

Surface tensions of membranes were determined by contact angle measurement. Hydrophilicity is the commonly used term in measuring water-solid surface interaction as a result of surface tension equilibrium (Young's Equation).The lower the contact angle, the more hydrophilic membrane will be. Contact angle is governed by the chemical composition as well as geometric structures of the surfaces. It was reported that water contact angle playing an important role in changing the permeation flux and fouling behavior of the membrane.[16,17]

The contact angles of the neat PVDF membrane and PVDF/$TiO_2$ mixed-matrix membrane prepared by PC-20 and P25 are shown in Figure 7. As depicted in Figure 7, the contact angle for PVDF membrane was reduced slightly with the incorporation of $TiO_2$ NPs via *in situ* colloidal precipitation method. This was mainly due to the $TiO_2$ NPs that were deposited on the PVDF/$TiO_2$ mixed-matrix membrane consisted of hydroxyl group which increased the membrane hydrophilicity.[18] This phenomenon had also been reported by many researchers, such

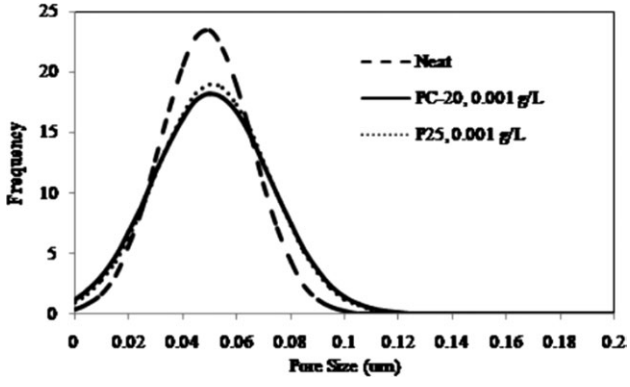


**Figure 5.** Pore size distribution of the PVDF/$TiO_2$ mixed-matrix membrane and neat membrane.

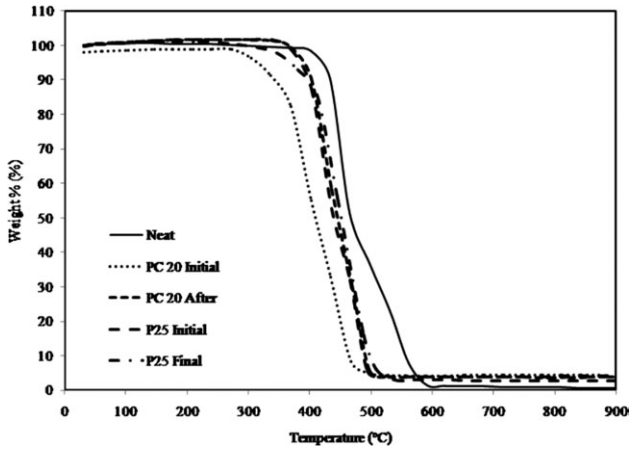


**Figure 6.** TGA thermograms of neat and PVDF/$TiO_2$ mixed matrix membrane before and after 6 h of membrane filtration process.

as Bae & Tak (2005) and Rahimpour et al. (2008) who found that the membrane surface contact angle decreased with the increased of entrapped $TiO_2$ concentration.[19,20]

In our study, less reduction of contact angle for PVDF/$TiO_2$ mixed-matrix membrane prepared by P25 compared with PC-20 has been observed, shows that PC-20 is relatively more hydrophilic than P25. Therefore, it was postulated that the hydrophilicity of PC-20 embedment could be relatively more significant compared with P25. This is most likely due to the different degree of crystallinity for each commercial $TiO_2$ nanopowders. The $TiO_2$ with anatase crystal structure has been reported by many researchers to have good characteristic in hydrophilicity.

### Streaming Potential

Figure 8 shows the zeta potentials of the neat membrane and PVDF/$TiO_2$ mixed-matrix membrane prepared at pH 7.0 and under the environment of 10 m*M* NaCl. The neat membrane and PVDF/$TiO_2$ mixed-matrix membranes obviously showed different electrokinetic properties at the same pH value. Although both membranes were negatively charged under $10^{-2}$ *M* NaCl solution environment, the zeta potential of the PVDF/$TiO_2$ mixed-matrix membrane was having higher value. The apparent zeta potential of the neat membrane and PVDF/$TiO_2$ mixed-matrix membrane prepared with PC-20 and P25 at concentration of 0.001 g/L were −8.505, −10.43, and −10.30 mV respectively. The negative charge of the neat membrane is due to the presence of dipolar polarization (orientation polarization) effect inherent by PVDF polar molecules on the base polymer and the preferential adsorption of negative chloride ions from the solution.[21]

Generally, the amphoteric behavior of mineral oxides is due to protonation and deprotonation of hydroxyl groups on the material surface.[22] The adsorption model of $H_2O$-$TiO_2$ in a stream atmosphere has been ascribed by Marrison (1980) who showed that the inequivalent adsorption of $H^+$ and $OH^-$ on the $TiO_2$ could takes place with $OH^-$ being adsorbed by the titanium cation and $H^+$ is adsorbed by the oxygen anion.[12,23] The adsorption of $H^+$ and $OH^-$ on the $TiO_2$ surface might not be equivalent and depends on the pH of the solution,[12] in which the surface net charge density and the surface potential of the membrane could be changed accordingly:

$$\text{In acidic medium, } (\text{Ti-OH})_{\text{surface}} + H_3O^+ \leftrightarrow \text{Ti-OH}_2^{\oplus} + H_2O \quad (2)$$

$$\text{In acidic medium, } (\text{Ti-OH})_{\text{surface}} + OH^- \leftrightarrow \text{Ti} - OH^- + H_2O \quad (3)$$

Equation (2) leads to a net positive charge on the surface of $TiO_2$ NPs due to the adsorbed $OH^-$ reacting with the $H^+$ in the solution; while eq. (3) leads to the net negative charge of $TiO_2$ NPs due to the adsorbed $H^+$ reacting with the $OH^-$ in the solution. The IEP of the $TiO_2$ NPs was reported to be ~pH

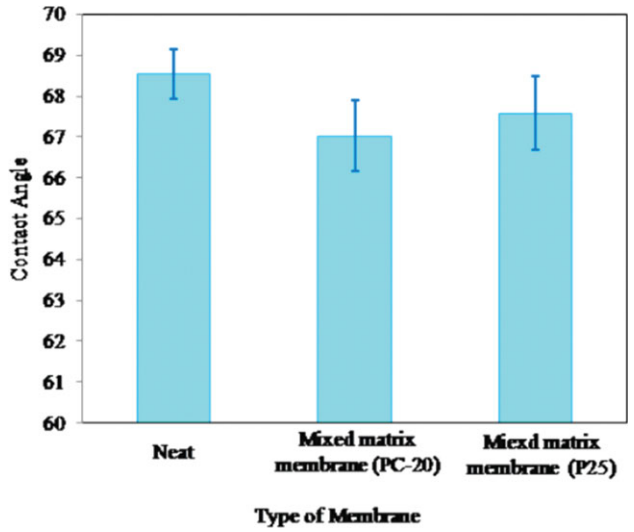


**Figure 7.** Contact angle of neat PVDF membrane and PVDF/$TiO_2$ mixed-matrix membranes. [Color figure can be viewed in the online issue, which is available at wileyonlinelibrary.com.]

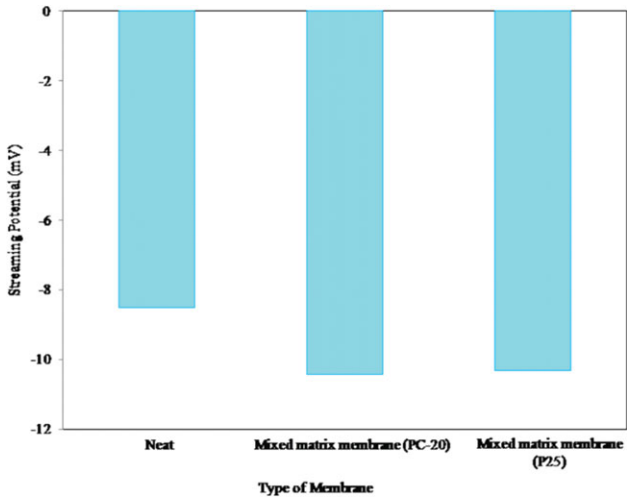


**Figure 8.** Effect of $TiO_2$ embedment on streaming potential with 1 m*M* $CaCl_2$ solution at pH 7.0. [Color figure can be viewed in the online issue, which is available at wileyonlinelibrary.com.]

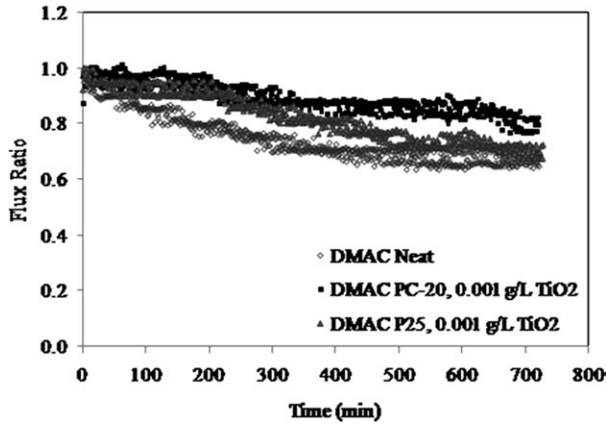


**Figure 9.** Effect of embedded $TiO_2$ on membrane fouling process. Operation conditions during the experiment: [HA] = 2 mg/L; $[Ca^{2+}]$ = 1 m*M* (as $CaCl_2$); pH 7.0; temperature = 25 ± 1°C; crossflow velocity = 4.0 L/h, operating pressure = 0.5 bar.

6.3,[24] so for NaCl solution at pH 7.0, which is greater than the IEP, the membrane would be negatively charged. The absolute value of the zeta potential for PVDF/$TiO_2$ mixed-matrix membranes is almost constant for both PC-20 and P25$TiO_2$ NPs. This is because, with the same concentration of $TiO_2$, the presence of counter-ions or charge density in the diffuse layer is almost the same, and thus results in similar value of streaming potential.

Streaming potential could provide useful information on HA fouling mechanism on membrane surface. Negatively charged $TiO_2$ particles on membrane surface demonstrate a strong ability to repeal HA from its aqueous solution. At pH 7, both HA and $TiO_2$ particles possess negatively charged surface which creates a strong electrostatic repulsion between HA and surface of $TiO_2$. Therefore, no significant absorption of HA on membrane surface was observed. The experimental results of HA absorption by Li et al. agrees with our postulation. According to Li et al., it was clear that the coverage of HA on the $TiO_2$ catalyst surface is obviously pH-dependent as the $TiO_2$ particles demonstrated a strong ability to adsorb HA on $TiO_2$ particles a low pH condition (pH < 3), but at pH 7 onwards, the absorption of HA become very difficult.[12] Therefore, increasing of membrane surface negative charge with the introduction of $TiO_2$ NPs is able to withstand fouling caused by adsorption.

### Effects of $TiO_2$ Embedment on Membrane Fouling

The common salts, which can be easily found in a variety of wastewaters, including monovalent ions ($Na^+$, $Cl^-$), divalent hardness cations ($Ca^{2+}$, $Mg^{2+}$), and divalent anions ($SO_4^{2-}$).[8] As reported by Wang et al., in the treatment of water solution containing HA, HA macromolecules was more readily form complexes with monovalent ions and change both humic substances and membrane surface charge which cause more severe fouling.[8] On the other hand, Srisurichan et al. claimed that at low pH, the dissociation of HA is lower and the available carboxyl functional groups for $Ca^{2+}$ are limited; thus, the complexation decreases. Their results show that the amount of coagulate was highest at pH 7 and decreased with decreasing pH.[25] This work was further proved by Hong and Elimelech[5] which showed the similar trend. In this work, we carried out the fouling test based on 1 mM $CaCl_2$ salt and solution pH of 7.

The performance of PVDF/$TiO_2$ mixed-matrix membrane on the HA fouling behavior are presented in Figure 9. The initial water fluxes for neat PVDF membrane, PVDF/$TiO_2$ mixed-matrix membrane embedded with PC-20 and P25 are 51.55, 53.03, and 53.32 L/$m^2$ h respectively showing that the mixed matrix membrane are relatively more hydrophilic. The observed flux increased upon integration of $TiO_2$ NPs can be explained by two possible reasons. During the exchange of $TiO_2$ NPs into the membrane surface, the PVDF membrane is exposed in the low pH HCl, in which the acid has been found to cause partial hydrolysis on the membrane surface and increase hydrophilicity, and hence increased the permeate water flux.[26] The other explanation may involve the water uptake characteristics of $TiO_2$ particles,[27] which are considered to be further contributions to the increase of permeate water flux.

Referring to Figure 9, for PVDF/$TiO_2$ mixed-matrix membrane with PC-20, the permeate flux was observed to be greater than PVDF/$TiO_2$ mixed-matrix membrane with P25, suggesting that PC-20 is more hydrophilic (higher anatase content) and had therefore promises a better HA fouling mitigation effect. This finding was in line with the work of Cao et al.[28] who claimed that, compared with the rutile $TiO_2$ NPs (average diameter ~30 nm), anatase $TiO_2$ NPs with a smaller diameter (~10 nm) are reported to have a better antifouling effect on the membrane prepared.

In addition to hydrophilic characters, PVDF/$TiO_2$ mixed-matrix membranes which possessed more negative charge on the top selective layer were also contribute in lowering fouling propensity. With the embedment of $TiO_2$ NPs into PVDF membrane polymeric matrix, it increased the zeta potential of the membrane surface. Sufficient electrostatic repulsion appears between highly charged PVDF/$TiO_2$ mixed-matrix membranes and HA aggregates alleviated the fouling phenomenon.

The fouling behavior is expressed in term of flux reduction based on flux ratio changes over time. One can see that with the presence of $CaCl_2$ salt in HA solution, neat PVDF membrane caused more severe fouling than PVDF/$TiO_2$ mixed-matrix membranes. Membrane fouling could be influenced by hydrodynamic conditions, such as permeation drag and back transport, and chemical interaction between foulants and membranes.[29] In order to relate the hydrophilicity with antifouling properties, the membranes were tested under similar hydrodynamic conditions and most important close to similar membrane physical properties. The later property could not be achieved by employing the conventional NPs embedment method but it could be achieved via our proposed surface coagulation method.

The result in Figure 9 clearly reveal the considerable flux decline, with a $J/J_0$ of 0.65, 0.70, and 0.82 for neat PVDF membrane, PVDF/$TiO_2$ mixed-matrix membrane embedded with PC-20 and P25, respectively after 12 h of operation (the end of each curve). These results suggest that the

incorporation of $TiO_2$ into PVDF membrane had successfully reduced the fouling propensity of the membrane towards HA. The dark brown deposit layer could be obviously observed on the neat membrane surface but to a less extent on the mixed matrix membrane.

The severe fouling of neat PVDF membrane by HA macromolecules occurs because the organic substances are transported to the membrane and accumulated near the membrane surface, which causes an increase in hydraulic resistance.[5,6,30,31] Since HA contains negatively charged carboxyl groups, divalent cations such as, $Ca^{2+}$ acts like a binding agent between the membrane surface and the negatively charged carboxyl groups of the HA.[32] As a result, the electrical repulsion between the membrane surface and the HA molecules was weakened[5,33] and adsorption occurred.

On the other hand, HA macromolecules appear to be less adsorbed onto the PVDF/$TiO_2$ mixed-matrix membrane as indicated by the less fouling phenomenon. This finding indicates that the hydrophilicity of PVDF membrane has been improved remarkably with the introduction of $TiO_2$ NPs on membrane surface via *in situ* colloidal precipitation method. The more hydrophilic of PVDF/$TiO_2$ mixed-matrix membrane than that the neat PVDF membrane is due to the higher affinity of $TiO_2$ towards water. Therefore, hydrophobic adsorption between HA macromolecules and PVDF/$TiO_2$ mixed-matrix membrane was reduced. Water molecules were attracted into the membrane matrix, forming a shielding layer to prevent fouling. These results are in consistent with other researcher findings[19,34,35,36] who observed that the modified membrane with addition of $TiO_2$ showed higher flux for sludge filtration than neat polymeric membrane.

## CONCLUSIONS

The effect of $TiO_2$ embedment into PVDF membrane polymeric matrix has been investigated for HA fouling phenomenon. The contact angle for PVDF membrane was slightly reduced and the surface zeta potential was increased with the incorporation of $TiO_2$ NPs. The results demonstrated that the PVDF/$TiO_2$ mixed-matrix membrane could be less prone to HA deposition as it exhibited a higher degree of hydrophilicity compared with neat PVDF membrane with the flux ratio for neat PVDF membrane, PVDF/$TiO_2$ mixed-matrix membrane embedded with PC-20 and P25 are 0.65, 0.70, and 0.82, respectively. PC-20 showed better antifouling properties compared to P25 due to its higher anatase polymorph. These properties render the membrane and HA with sufficient electrostatic repulsion and therefore enhanced the fouling mitigation. The effect of $TiO_2$ NPs on membrane antifouling could be realized only if the membranes were compared with the same basis (hydrodynamic and physical properties) which can be realized using the proposed colloidal precipitation method.

## ACKNOWLEDGMENTS

The authors wish to the thank the sponsors of this project for their financial supports, namely Universiti Sains Malaysia (USM) Research University Grant (1001/PJKIMIA/811172), Malaysia Toray Science Foundation (MTSF) Science and Technology Research Grant (304/PJKIMIA/6050179/M126), MOSTI e-Sciencefund (305/PJKIMIA/6013604) and USM Membrane Cluster.

## REFERENCES

1. Kimura, K.; Hane, Y.; Watanabe, Y.; Amy, G.; Ohkuma, N. *Water Res.* **2004**, *38* (14–15), 3431.
2. Yamamura, H.; Chae, S.; Kimura, K.; Watanabe, Y. *Water Res* **2007**, *41*, 3812.
3. Nyström, M.; Rouhomäki, K.; Kaipia, L. *Desalination* **1996**, *106*, 79.
4. Wei, Y.; Zydney, A. L. *J. Membr. Sci.* **1999**, *157*, 1.
5. Hong, S. K.; Elimelech, M. *J. Membr. Sci.* **1997**, *132*, 159.
6. Braghetta, A.; DiGiano, F. A.; Ball, W. P. *J. Environ. Eng. ASCE* **1998**, *124*, 1087.
7. Kabsch-Korbutowicz, M.; Majewska-Nowak, K.; Winnicki, T. *Desalination* **1999**, *126*, 179.
8. Wang, Z.; Zhao, Y.; Wang, J.; Wang, S. *Desalination* **2005**, *178*, 171.
9. Lee, N.; Amy, G.; Crouse, J.; Buison, H. *Water Res.* **2004**, *38*, 4511.
10. Lee, E. K.; Chen, V.; Fane, A. G. *Desalination* **2008**, *218*, 257.
11. Li, J. B.; Zhu, J. W.; Zheng, M. S. *J. Appl. Polym. Sci.* **2007**, *103*, 3623.
12. Li, X. Z.; Fan, C. M.; Sun, Y. P. *Chemosphere* **2002**, *48*, 453.
13. Cho, J. W.; Amy, G.; Pellegrino, J. *J. Membr. Sci.* **2000**, *164*, 89.
14. Kwak, S. Y.; Kim, S. H.; Kim, S. S. *Environ. Sci. Technol.* **2001**, *35*, 2388.
15. Teow, Y. H.; Ahmad, A. L.; Lim, J. K.; Ooi, B. S. *Desalination* **2012**, *295*, 61.
16. Gau, H.; Herminghaus, S.; Lenz, P.; Lipowsky, R. *Science* **1999**, *283*, 46.
17. Li, M.; Zhai, J.; Liu, H.; Song, Y.; Jiang, L.; Zhu, D. *J. Phys. Chem. B* **2003**, *107*, 9954.
18. Yuliwati, Y.; Ismail, A. F. *Desalination* **2010**, *273*, 226.
19. Bae, T. H.; Tak, T. M. *J. Membr. Sci.* **2005**, *266*, 1.
20. Rahimpour, A.; Madaeni, S. S.; Taheri, A. H.; Mansourpanah, Y. *J. Membr Sci.* **2008**, *313*, 158.
21. Burns, D. B.; Zydney, A. L. *J. Membr. Sci.* **2000**, *172*(1-2), 39.
22. Regazzoni, A. E.; Blesa, M. A.; Maroto, A. J. G. *J. Colloid Interf. Sci.* **1983**, *91*, 560.
23. Marrison, S. R. In Electrochemistry at Semiconductor and Oxidation Metal Electrodes; Plenum Press, New York, **1980**.
24. O'Shea, K. E.; Cardona, C. *J. Photoch. Photobio. A* **1995**, *91*, 67.
25. Srisurichan, S.; Jiraratananon, R.; Jane, A. G. *Desalination* **2005**, *174*, 63.

26. Kulkarni, A.; Mukherjee, D.; Gill, W. N. *J. Membr. Sci.* **1996**, *114*, 39.
27. Khare, S. Presented at International Conference on Polymer Characteristics (POLYCHAR-8). University of North Texas, Denton, TX. **2000**, 11–14.
28. Cao, X.; Ma, J.; Shi, X.; Ren, Z. *Appl. Surf. Sci.* **2006**, *253*, 2003.
29. Maximous, N.; Nakhla, G.; Wan, W. *J. Membr. Sci.* **2009**, *339* (1–2), 93.
30. Wei, W.; Zydney, A. L. *Environ. Sci. Technol.* **2000**, *34*, 5043.
31. Cho, J. W.; Amy, G.; Pellegrino, J. *Water Res.* **1999**, *33*, 2517.
32. Jucker, C.; Clark, M. M. *J. Membr. Sci.* **1994**, *97*, 37.
33. Schäfer, A. I. Natural Organics Removal Using Membranes, PhD Thesis, University of New South Wales, **1999**.
34. Bae, T. H.; Kim, I. C.; Tak, T. M. *J. Membr. Sci.* **2006**, *275*, 1.
35. Kim, S. H.; Kwak, S. Y.; Sohn, B. H.; Park, T. H. *J. Membr. Sci.* **2003**, *211*, 157.
36. Li, Y. Y.; Shen, H. M.; Xu, Z. L. *J. Appl. Polym. Sci.* **2009**, *113*, 1763.